WORLD METEOROLOGICAL ORGANIZATION

2nd Antarctic Climate Forum Consensus Statement

Summary of the Antarctic and Southern Ocean November 2025 – April 2026 season and outlook for June – August 2026

2 – 3 June 2026

Contents

Introduction to the Antarctic Climate Forum Consensus Statement

Surface annual average temperatures are rising in most of the regions of the Antarctic continent and adjacent seas of the Southern Ocean (Figure 1), changing the state of Antarctic glaciers, shelf ice and impacting global sea level. Monitoring, understanding and predicting the climatic conditions in the region is therefore important due to the links to and direct impacts on both current and future local, regional and global climate and wider environmental conditions.

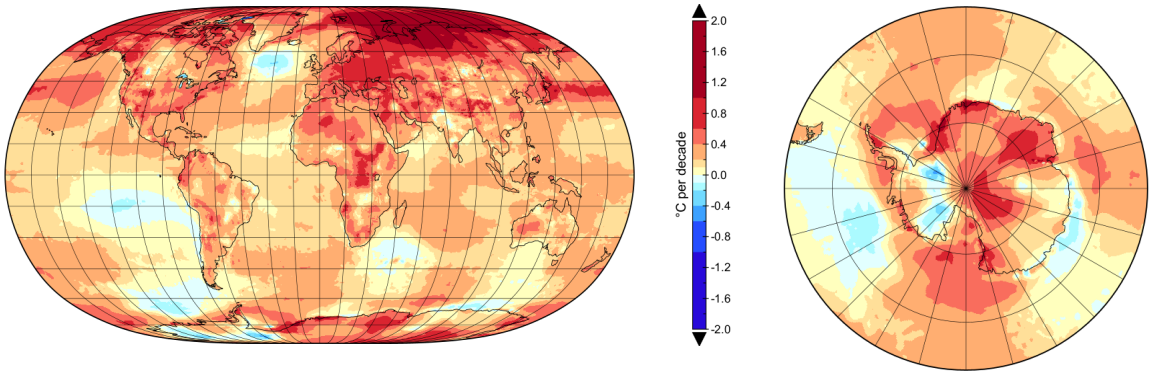

Figure 1: Global (with cutout for Antarctic region) annual surface temperature trend (°C/decade) for 1996-2025 period. Graphics produced by the AARI. Data source: ERA5 monthly averaged surface air temperature at 2m level.

The Antarctic Regional Climate Centre Network (AntRCC-Network) has been initiated as a World Meteorological Organization (WMO) centre of excellence to assist WMO Members to develop and deliver climate services and products. The AntRCC-Network fosters collaboration amongst Meteorological Services and researchers, in the Antarctic, to meet climate-related decision-making needs among stakeholders across the region.

The Antarctic Climate Forum (AntCF) is convened by the AntRCC-Network under the auspices of the WMO, as a fundamental platform to promote cooperation and information sharing on the weather and climate that occurred in the most recent season as well as forecasts for the season ahead. At the inaugural AntCF session, held at the British Antarctic Survey in Cambridge, UK, in January 2026, it was recommended that AntCF should be conducted twice a year: before the launch of and at the conclusion of the austral summer expedition season, which typically runs October-March.

A main product of AntCFs is a Consensus Statement for the Antarctic and Southern Ocean, which synthesises observations, historical trends, forecasts, and in doing so, includes regional expertise. These statements include a review of the major climate features of the previous season and outlooks for the upcoming season for temperature, precipitation, sea-ice and sea surface temperature.

This Consensus Statement is an outcome of the 2nd session of the AntCF, held online 2 – 3 June 2026. The event was coordinated by the National Centre for Polar and Ocean Research (NCPOR), India and contains a review of WMO Essential Climate Variables (ECV) for November 2025 to April 2026 season, and the forecast for the June – September 2026 season.

Highlights for decision making

Temperature

Data from model reanalysis products for the November 2025 to April 2026 period indicate that while record temperatures were approached in many regions, they were not spatially uniform across all Antarctic regions. The seasonal features were characterized by large positive anomalies over the East Antarctica Indian, Pacific and Antarctic Peninsula sectors, and the adjacent areas of the Southern Ocean. Negative anomalies were observed within the Plateau - Ross Sea and East Antarctica Atlantic sectors. These findings from model reanalysis products are in good agreement with observations performed at staffed ground stations.

Predictions for the June-August 2026 period show that much of the Southern Ocean in the Antarctic RCC's area of interest has 50-80% probabilities of above normal temperatures, apart from a small region in the Amundsen Sea where a 50-60% chance of below-normal temperatures is predicted. Temperatures across much of the continent show a 40-60% chance of being normal, and greater than 70% of chance of being warmer than normal along the western Antarctic Peninsula.

Precipitation

Reanalysis results for the November 2025 – April 2026 period for precipitation anomalies over sea ice and surrounding waters were generally weak and spatially varying. The East Antarctic area, including the Cooperation and Davis Seas and Wilkes Land, as well as the West Antarctic Ellsworth and Marie Byrd Lands were characterised by persistently higher precipitation, while drier conditions occurred over the East Antarctic Atlantic and Plateau – Ross Sea regions. Ground based observations indicate that positive precipitation anomalies were dominant during the Nov-Apr 2026 period at the north-eastern Peninsula stations and at the southern Weddell Sea. Conversely, pronounced negative anomalies (both precipitation and snow) occurred north-east of the tip of the Peninsula.

Precipitation predictions for the June-August 2026 period are largely for above-normal anomalies. The oceanic sector from the Antarctic Peninsula clockwise through to the Ross Sea show 50-70% probabilities of above-normal precipitation. The remaining Amundsen Sea region, particularly north of 60S, however shows a 40-50% probability of below-normal precipitation for the JJA period. Over the continent, 40-60% probabilities of above-normal precipitation extend across the entire Antarctic Peninsula and East Antarctic-Atlantic region. 40-50% probabilities of above normal precipitation occur over the high interior and closer to the coast between 130E clockwise through to 130W. 40-50% probabilities of below-normal precipitation is indicated in the East Antarctic interior between 60-110E.

Sea-ice

The nominal sea ice edge is considered to be represented by the 15% sea ice concentration contour. The 2026 annual minimum net sea-ice extent was reached during 22-26 February with a total area close to 2.6-2.8 million square km, ranking 16th lowest on record for the period 1979-2026. Special features of the seasonal variability of the sea-ice conditions included southmost position of the ice edge during the spring melt in the seas of the Indian and eastern part of the Pacific sector with opposite northernmost ice edge position for parts of the Atlantic sector, drastic reduction of sea-ice at the peak of summer melt in most of the areas of the Indian and Pacific sectors with opposite median ice cover in West Weddell and Amundsen seas.

Sea Ice predictions for September 2026 display a wide latitudinal spread (i.e. where the forecast ice edge position has the most uncertainty) in the Pacific and Atlantic sectors running clockwise from 150W to 30E. Slight positive ice concentration anomalies relative to the ERA5 median 1991-2020, and subsequently a more northern ice edge position and increased extent are predicted for the Pacific and Atlantic Regions (Weddell Sea). Negative ice concentration anomalies, with reduced extent and a more southward position of the ice edge are predicted for the Indian Ocean Region (Cooperation and Davis seas). A weak dipole of ice concentration anomaly is represented in the Pacific (Ross Sea) Region at 160E and 150W.

Understanding the Consensus Statement

This consensus statement includes the seasonal summary and forecasts verification for surface air temperature, precipitation, sea-ice and sea surface temperature for the November 2025 to April 2026 period; and their outlook for upcoming June to August 2026 period, as well as sea ice concentration prediction for September 2026. Figure 2 shows the five regions defined by the AntRCC-N members on the basis of accepted regional practices to capture the different geographic features and environmental factors influencing temperature, precipitation and other Antarctic ECVs, along with the major land and ocean geographical features selected for description of the products.

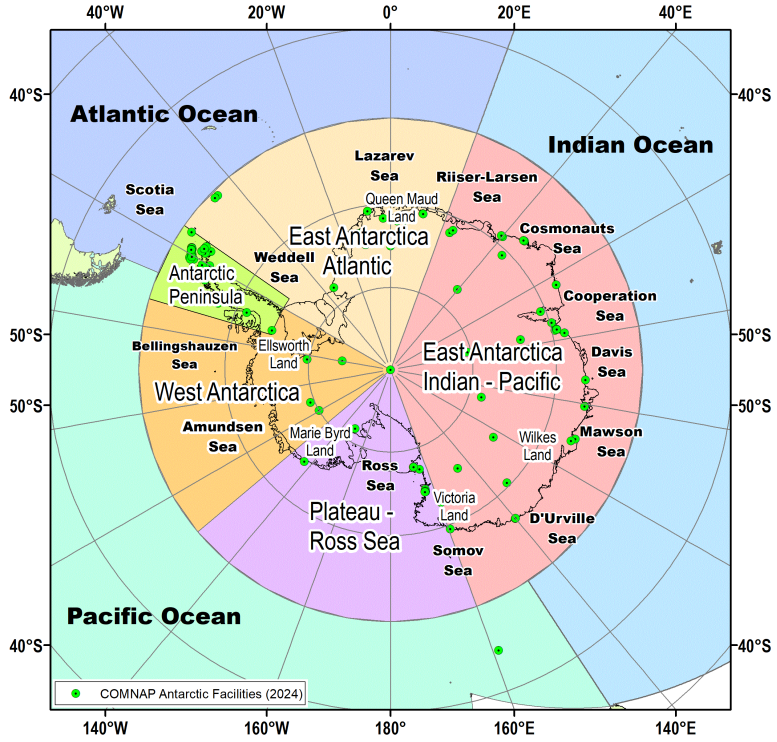

Figure 2: Five defined AntRCC-N regions and major land and ocean geographical features in Antarctica selected by the network members for practical purposes for seasonal summaries and outlooks. Graphics produced by AARI.

Seasonal summaries for temperature, precipitation, sea-ice and other Antarctic ECVs are based on a synthesis of routine manual and automated (in-situ and remotely sensed) observations, sea-ice analysis from national ice services, and the ERA5 reanalysis products from the Copernicus Climate Change Service. Anomalies of the parameters are given in most cases for the WMO reference period 1991-2020, which allows to efficiently underline the most recent interannual variability.

The seasonal forecasts for temperature and precipitation are based on up to fifteen models from WMO Global Producing Centres for Seasonal Prediction (GPCs-SP) and consolidated by the WMO Lead Centre for Seasonal Prediction Multi-Model Ensemble (LC-SPMME). In terms of model skill (i.e., the ability of the climate model to simulate the observed seasonal climate), a multi-model ensemble (MME) approach overlays all the individual model performances. This provides a forecast with higher confidence in the regions where different model outputs/results are consistent, versus a low confidence forecast in the regions where the models don't agree. The MME approach is a methodology well-recognized by the WMO to be providing the most reliable objective forecasts.

Temperature

Summary

Changes in surface air temperature drive or indicate the onset of changes for other parameters of the Antarctic environment. Data and products presented below indicate that the spring – summer – autumn 2025/26 (November to April) period was characterised as one of the warmest on record across the Antarctic region. Reanalysis and ground-based observations indicate that while record temperatures were approached, they were not spatially uniform across all Antarctic regions (see Figure 3 and Table 1). The seasonal features were characterised by considerable positive anomalies over the East Antarctica Indian – Pacific and Antarctic Peninsula sectors, and their adjacent areas of the Southern Ocean. Areas of negative anomalies were observed within the Plateau - Ross Sea and East Antarctica Atlantic sectors. A comparative analysis with the conditions observed during the same period of 2024/25 (both reanalysis and surface observations) indicates high contrast: 2024/25 was characterised by less widespread negative anomalies during November to January but predominant negative anomalies in East Antarctica Indian – Pacific during February to April.

Seasonal review: November 2025 – April 2026

Based on reanalysis, the austral spring - summer 2025/2026 period was characterised by positive anomalies across the largest part of continent. However persistent negative anomalies characterized a broad band that crosses the entire continent from the Atlantic to the Ross Sea, including the South Pole. This band is very evident and continuous during the months of NDJ and less marked and discontinuous in the early months of 2026. In the Southern Ocean, alternate negative and positive anomalies were visible (Figure 3a).

At the monthly scale, the zones of negative anomaly tend to not be stable across the continent. In November, they persist only over the Peninsula. By December the negative anomaly over the Peninsula shifts south-east along with a localised area of negative anomalies extending along the dateline from the Ross Sea all the way up to the Atlantic and Indian Sectors. Similar negative anomalies were present in the Ross Sea during January and to a greater extent during April. The month of April exhibits a dipole structure, with positive anomalies over the Peninsula region and negative anomalies over West Antarctica, Ross Sea and Wilkes Land. Ranking of the anomalies indicate that the Antarctic Peninsula and East Antarctica experienced close to the strongest warming since 1950 (Figure 3a bottom).

Direct measurements at about 30 selected staffed stations are in good agreement with reanalysis findings strengthening our confidence in the trends just described. Across the early summer period - November to January, temperatures were consistently above average across all Australian Antarctic stations (Casey, Davis and Mawson), particularly in November and January when both mean maximum and minimum temperatures were above average (Figure 3b). December had maximum temperature at or above average across all Australian Antarctic

stations, although Mawson recorded slightly below average minimum temperatures. Conversely, Casey recorded its warmest December mean temperature of 0.1 °C and mean minimum temperature of -2.1 °C since 2005. Between February to April, temperature was varied across the Australian Antarctic stations. During February, above average mean maximum and minimum temperatures were observed at Casey recording the station's warmest February mean maximum and mean temperatures since 1993 and 2004, of 1.5 °C and -1.2 °C respectively, and below average mean conditions at Davis and Mawson. In contrast, Casey recorded below average temperatures in March, whereas Davis and Mawson observed above average conditions, which resulted in Davis observing its highest March mean maximum, minimum and mean temperatures of -3.4 °C, -8.2 °C, and -5.7 °C since 1959 and Mawson recording its equal highest March mean maximum and mean temperatures of -5.1 °C and -8.1 °C, since 1991 and 2005 respectively, and its highest mean minimum temperature of -11.2 °C since 2005. April saw consistently above-average mean maximum and minimum temperatures across all the Australian Antarctic stations.

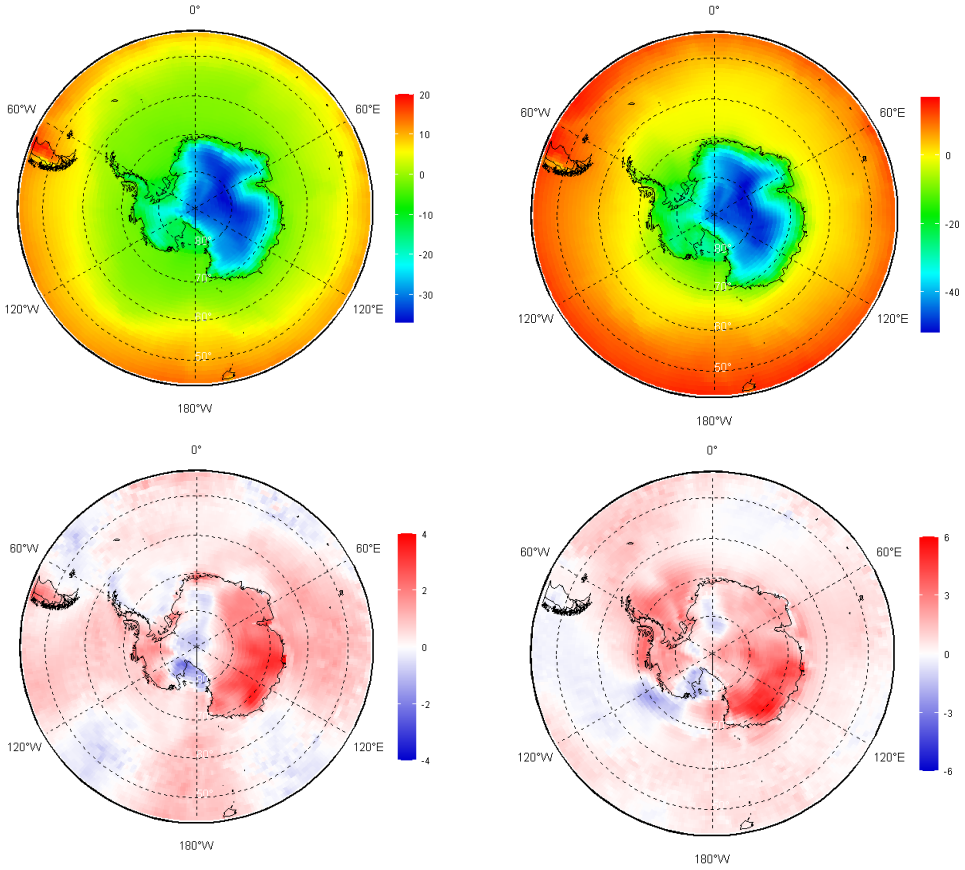

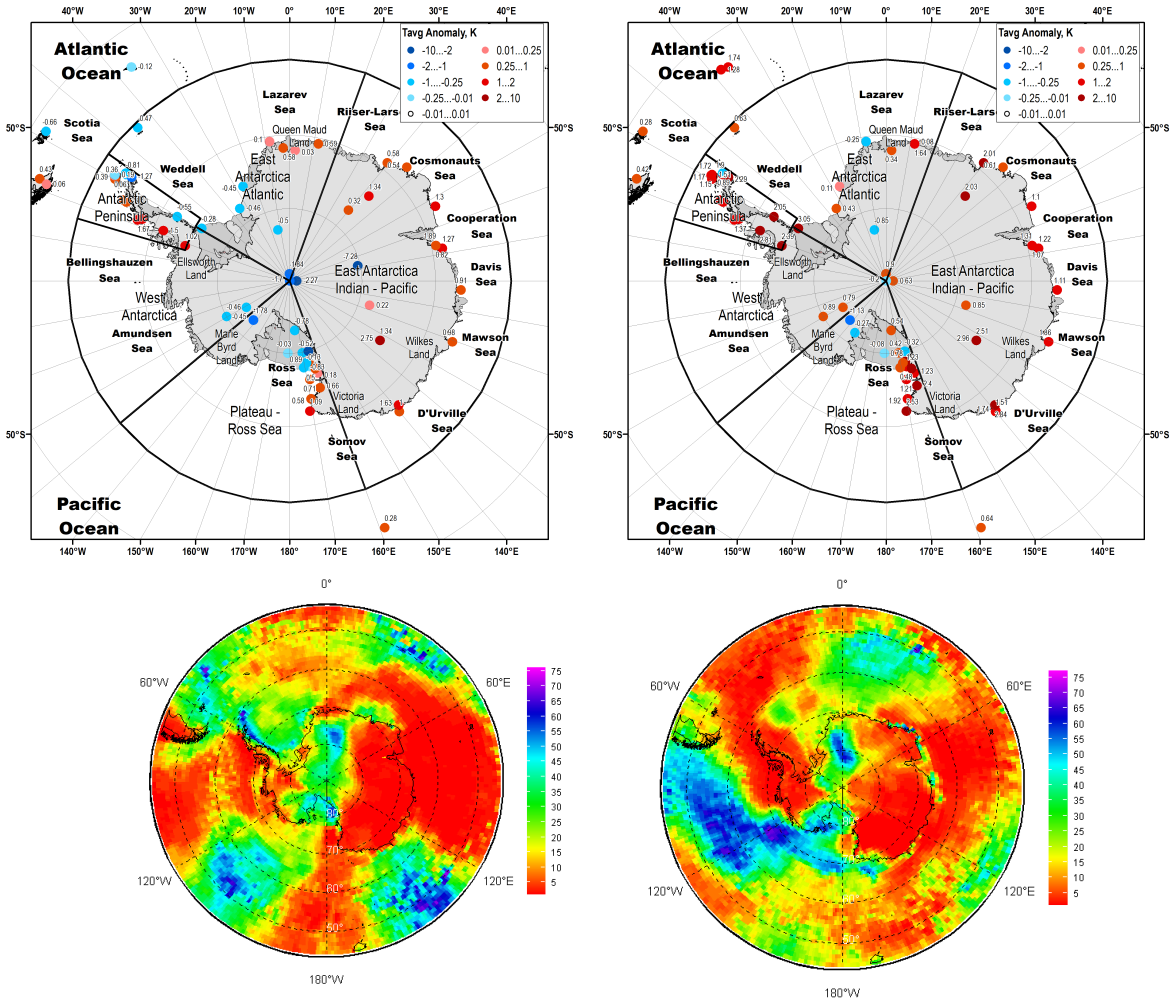

November 2025 – January 2026 February – April 2026

Figure 3a – Surface air temperature (2m, °C) seasonal averages (top), anomalies relative to 1991-2020 period based on reanalysis (2nd row) and direct measurements at the staffed stations (3rd row) and ranks relative to 1950-2025/2026 period (bottom) with 1 being the warmest (bottom). Data source: ERA5, READER national repositories, WMO GTS, graphics produced by AARI. Left/Right column depicts averages for November-January 2026/February-April 2026.

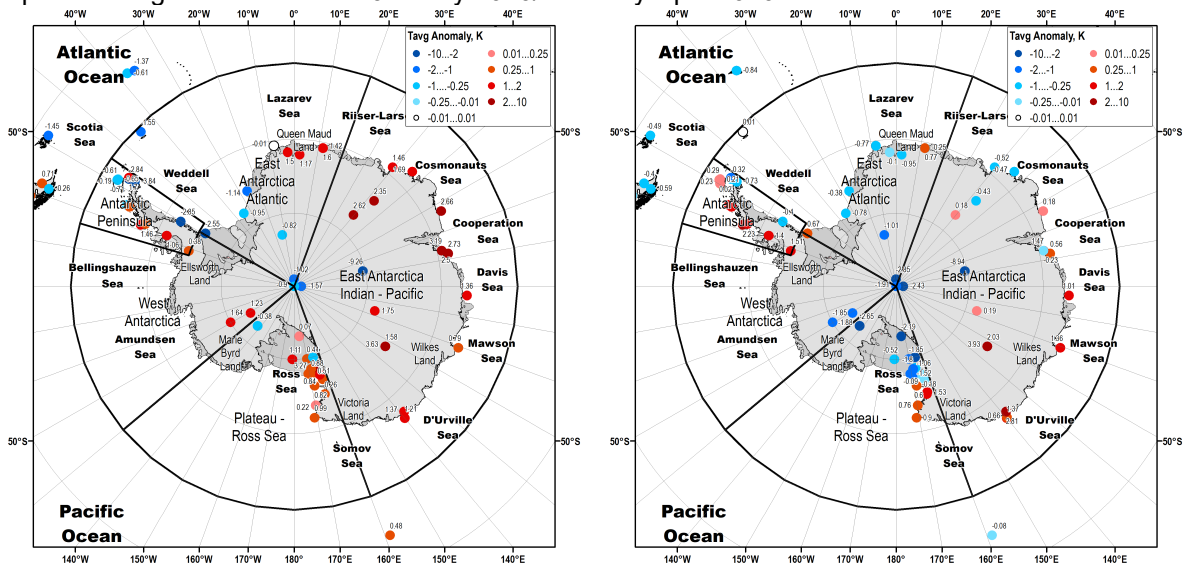

November December

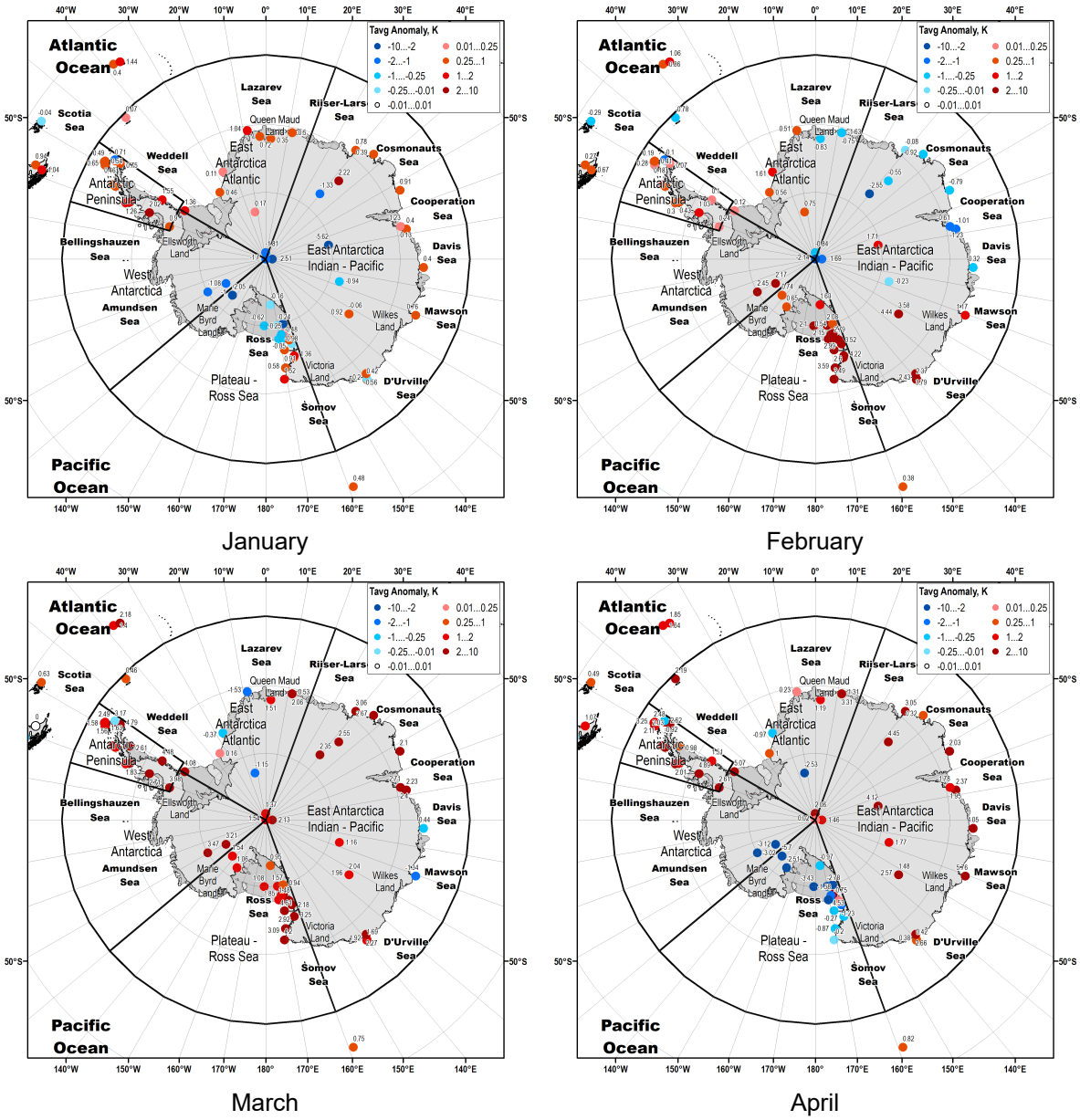

Figure 3b – Surface air temperature (2m, °C) monthly anomalies relative to 1991-2020 period for November 2025 – April 2026. Data source: READER national repositories, WMO GTS. Graphics produced by AARI.

Table 1 – Surface air temperature anomalies (°C; reference period 1991-2020) and consecutive ranks (reference period 1957-2025/2026) for November 2025 – April 2026 based on observations at about 30 selected staffed stations and grouped by five regions. Extreme positive anomalies (ranks 1-5) marked bold red, negative anomalies marked blue.

Period	Peninsula		East Antarctica Atlantic		East Antarctica Indian-Pacific		Plateau-Ross Sea		West Antarctica	
	anomaly	rank	anomaly	rank	anomaly	rank	anomaly	rank	anomaly	rank
2025-11	**-0.81**	51	**-0.33**	30	**2.00**	**2**	0.91	11	1.16	11
2025-12	0.61	7	**-0.66**	53	0.91	16	**-0.02**	34	**-1.61**	43
2026-01	**0.71**	**4**	0.45	21	0.65	25	**-0.23**	39	**-0.96**	34
2026-02	0.11	26	**-0.03**	34	0.31	24	**2.52**	**3**	2.68	9
2026-03	**1.92**	**2**	0.55	28	1.05	15	1.60	11	**4.46**	**2**
2026-04	**2.12**	**5**	1.26	25	2.82	8	0.43	30	**-3.64**	48

Verification of FMA (February – March – April) 2026 forecast

Only a subjective verification has been undertaken. The probabilistic (Figure 4 left) and deterministic (Figure 4 middle) outlooks issued on the 15th January for the FMA 2026 period largely reflect the above normal temperatures analysed by the ERA5 reanalysis (Figure 4 right). The negative SAT anomalies Amundsen Sea were forecast. The higher probability of below normal SAT in the Weddell and Somov Sea regions did not eventuate for the 3 months period, but it is noteworthy that strong negative temperature anomalies were analysed in the Somov Sea in April (not shown), in alignment with the FMA probabilistic and deterministic forecasts.

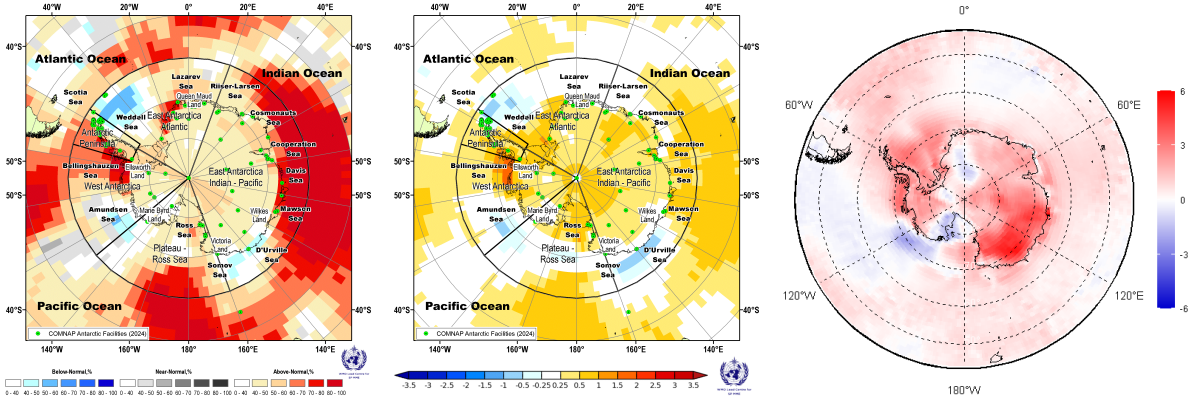

Figure 4 – FMA (February – March – April) 2026 surface air temperature (2m): probabilistic (left) and deterministic (middle) outlooks of 15 January 2026 run by WMO LC-LRFMME, and anomaly reanalysis relative to 1991-2020 period (right) by ERA5 reanalysis. Data source: WMO LC-LRFMME (outlook), ERA5 (reanalysis), graphics produced by AARI.

Seasonal Outlook: JJA (June – July – August) 2026

The June-August 2026 outlook predicts 50-80% probabilities of above normal SAT's over much of the Southern Ocean apart from a small region in the Amundsen Sea where a 50-60% chance of below-normal SAT is predicted. Over the continent, all of the East Antarctic- Atlantic region has 40-60% probability of above normal SAT's. A large area of the East-Antarctic Indian-Pacific region has a 40-50% probability of above-normal SATs, whilst no clear signal is present in much of the continental region between 60-120E. The western Antarctic Peninsula

has above 70% chance of above normal SATs. Monthly probabilities indicate that the cold anomalies in the Amundsen seas are less likely in August.

Information on the skill of the MME forecast for the surface air temperature and precipitation is provided in Annex 2. It appears that overall, the Antarctic Polar region generally has poorer forecast skill than most other parts of the globe. For JJA SAT's, there's some weak skill in the Pacific region between the Ross Sea and the Antarctic Peninsula, but for precipitation skill is generally poor across most of the continent.

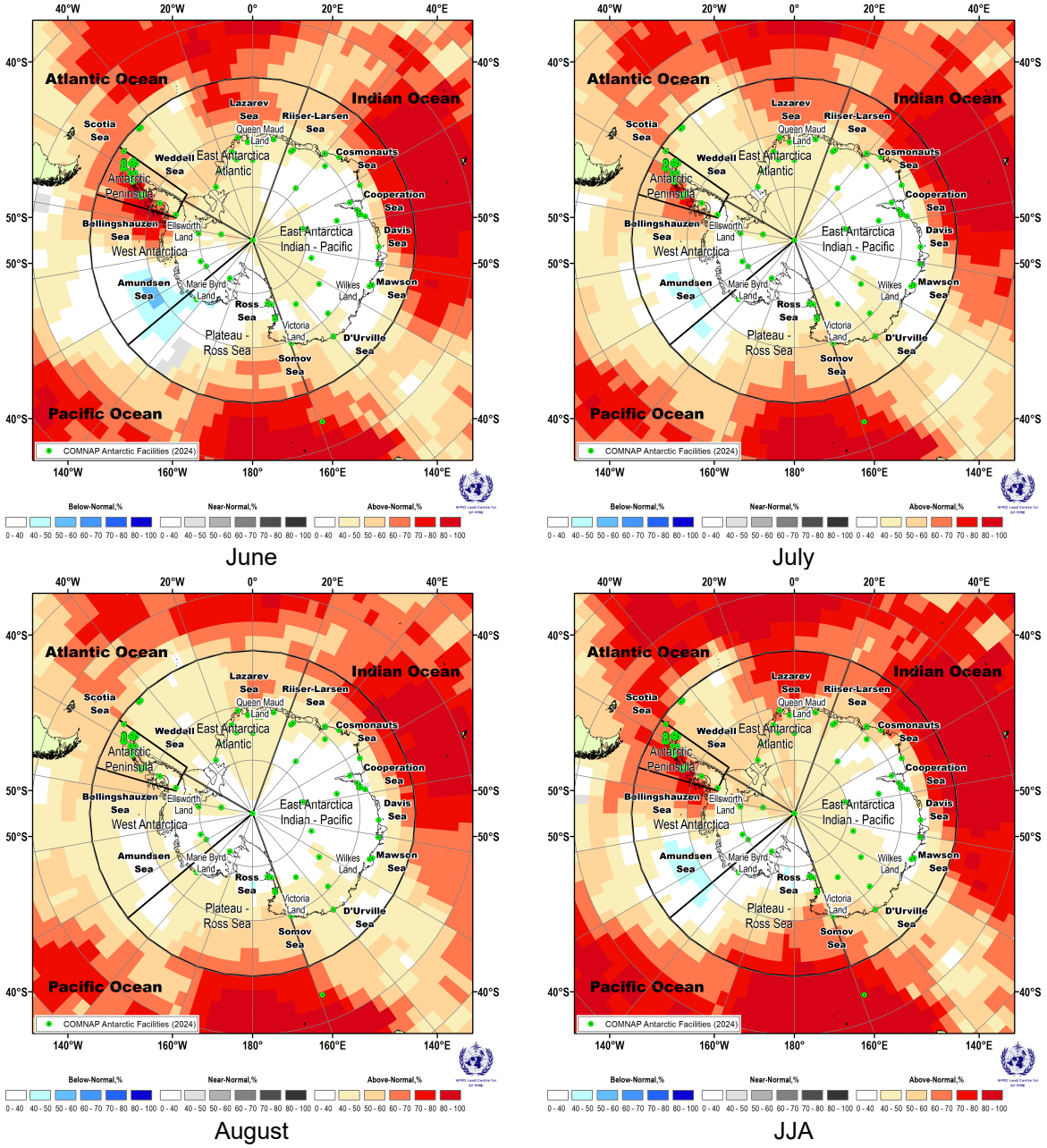

Figure 5 – Surface air temperature (2m) anomaly (relative to 1991-2020 period) seasonal probabilistic outlook for June, July, August and JJA 2026. Data source: WMO Lead Centre for Seasonal Prediction Multi-Model Ensemble (wmolc.org) forecast (11 GPCs-SP models) using data of 14 May 2026, graphics produced by AARI.

The JJA forecast has many similarities with the FMA ERA5 reanalysis (Figure 4 right) – i.e. negative anomalies in the Ross/Amundsen seas and a stronger tendency for above normal temps in East Antarctica.

Precipitation

Summary

Precipitation measurements in Antarctica are very challenging, much more so than temperature observations. The main reason for the very few available observations is the lack of automatic and unattended measurements in recent years. The general summary picture presented below arise only from model-produced reanalysis products with ground staffed observations available to give details only over the Antarctic Peninsula.

Seasonal review: November 2025 – April 2026

Based on the ERA5 reanalysis precipitation anomalies over the coastal and polar ocean regions, the Nov-Apr period included both drier and 'wetter' conditions relative to 1991-2020 period (figure 6). Maximum positive precipitation anomalies were noted in the East Antarctic Indian - Pacific sector between 50 and 140E with ranks pointing to one of the 'wettest' years (Figure 6 bottom). A patch of positive precipitation anomaly was also noticed west of the Antarctic Peninsula. Variable patches of 'wet' and dry anomalies were noticed in the ocean throughout the whole past season.

Direct observations at the stations indicate that in the early summer period, precipitation across the Australian Antarctic stations (excluding Mawson) ranged from average to above average. Above average precipitation was observed at Casey and Davis in November and January, while conditions in December were closer to average. Moving into late summer and early autumn, precipitation was more variable. At Casey, precipitation was average in February and April, and below average in March. At Davis, precipitation was above average in February and March, before dropping below average in April.

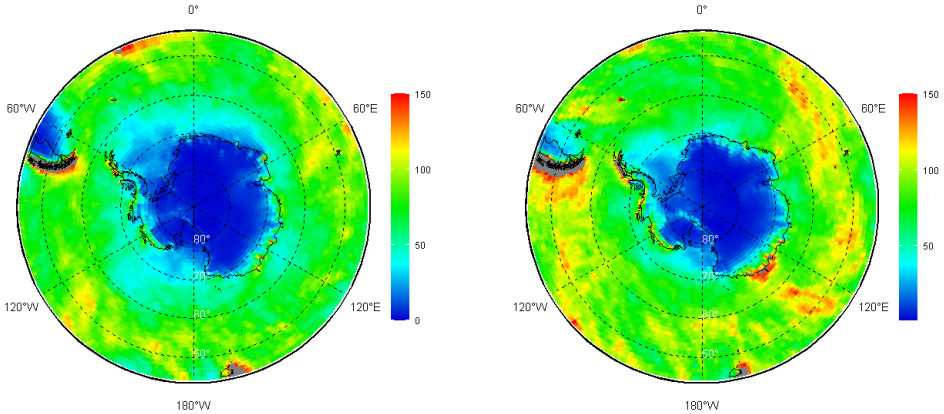

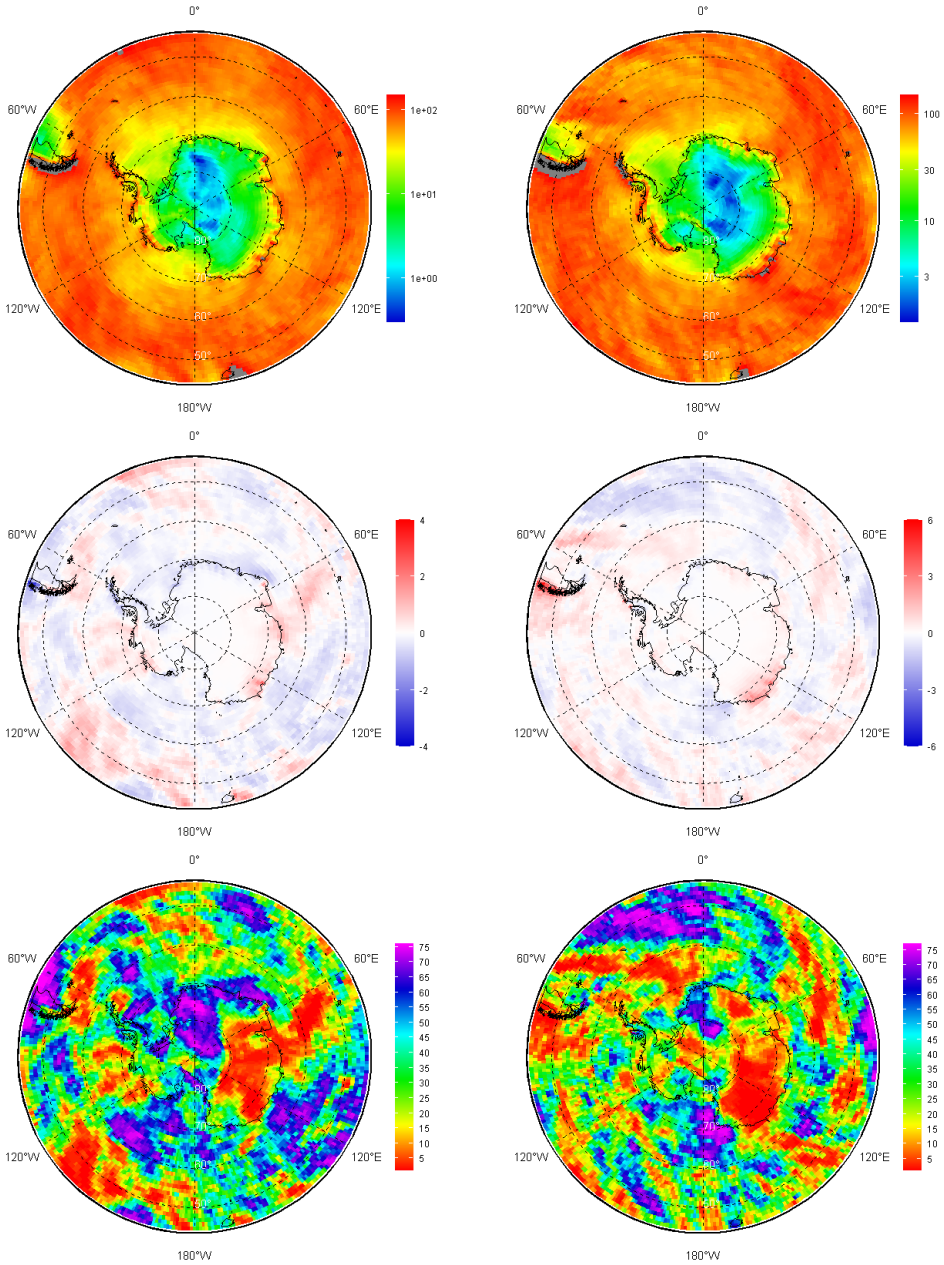

November 2025 – January 2026 February – April 2026

Figure 6a – Surface precipitation seasonal averages in mm/month in linear (top row) and log scales (second row), anomalies in mm/month relative to 1991-2020 period (third row), ranks relative to 1950-2025/2026 period with 1 being the wettest (bottom row). Data source: ERA5, graphics produced by AARI.

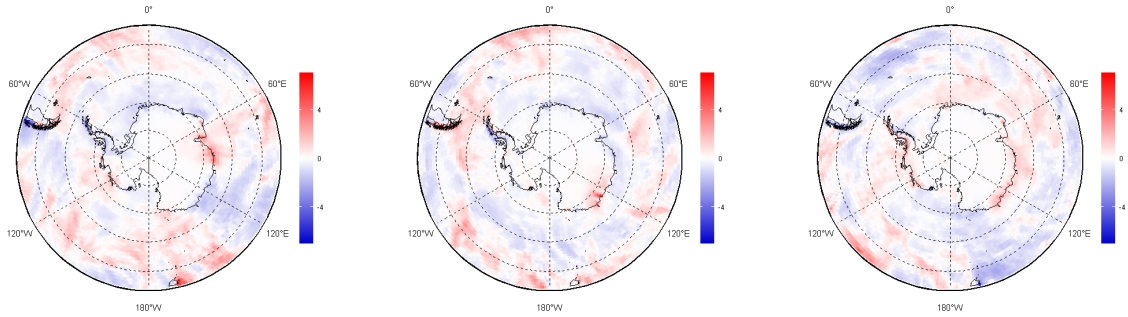

November 2025 December 2025 January 2026

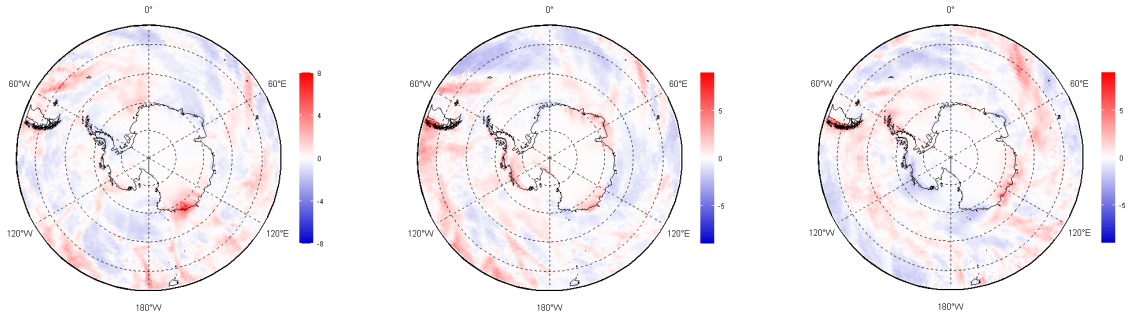

February 2026 March 2026 April 2026

Figure 6b – Surface precipitation monthly anomalies in mm/month relative to 1991-2020 period. Data source: ERA5, graphics produced by AARI.

Precipitation and Snow in the Antarctic Peninsula

Throughout the past season the frequency of precipitation days exhibited high spatial and temporal variability. Positive precipitation anomalies were dominant during the summer months at the north-eastern Peninsula stations and at the southern Weddell Sea. Conversely, pronounced negative anomalies (both precipitation and snowfall frequency) occurred north-east of the tip of the Peninsula (Orcadas station) (Figure 6c). This analysis is based on *in situ* observations conducted at seven research stations (Esperanza, Orcadas, Carlini, Great Wall, Marambio, San Martín, and Belgrano II). Although these records are from high-quality local observations, it should be noted that they represent specific point locations across the Peninsula.

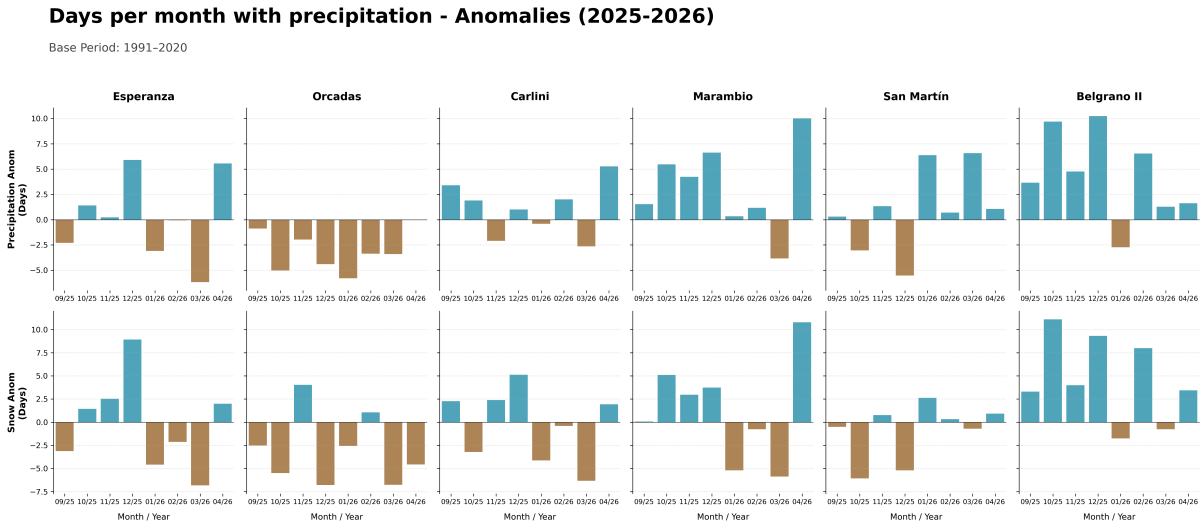

Figure 6c – Precipitation and snow frequency anomalies for 2025 (relative to 1991-2020, unit: days) in the Antarctic Peninsula.

Additional information for the ground instrumental precipitation measurements using Micro Rain Radar technique (MRR; K-band,24GHz) deployed at China's Antarctic Great Wall Station at northmost part of the Peninsula is provided in Annex 1.

Verification of the February – April 2026 precipitation forecast

Only a subjective verification has been undertaken (figure 7). The probabilistic forecast for FMA 2026 indicated 50-60% chance of above normal precipitation along the Antarctic Peninsula and adjacent Ellesworth Land as well as much of the Indian and Pacific Ocean coastal region. The remaining Antarctic regions indicated an equal mix of below, near and

above-normal probabilities. These positive anomalies did eventuate according to the ERA5 reanalysis.

However, ERA5 reanalysis shows near record positive precipitation anomalies in the interior of East Antarctica, particularly in the Indian Region, which we're not signalled in the forecast. Negative precipitation anomalies off the Ross Sea also occurred where there was an equal mix of below, near and above-normal probabilities

The large region of 50-60% probability of above normal precipitation forecast for the ocean sector south of approximately 58S does not subjectively match with the ERA5 reanalysis for that same region. It may be noted that these regions also exhibited enhanced probability of warming as well, whereas zero probability for precipitation was noticed in locations where cold temperature anomalies were present (Figure 4).

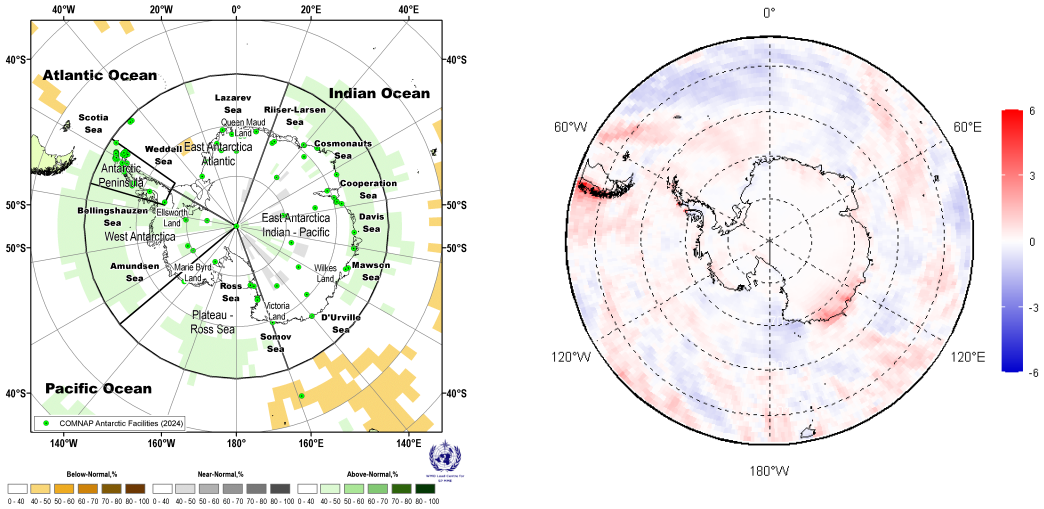

Figure 7 – FMA (February – March – April) 2026 surface precipitation probabilistic outlook (left) of 15 January 2026 by WMO LC-LRFMME and anomaly reanalysis in mm/month relative to 1991-2020 period (right) by ERA5 reanalysis. Data source: WMO LC-LRFMME (outlook), ERA5 (reanalysis), graphics produced by AARI.

Seasonal Outlook: JJA (June – July – August) 2026

From the Antarctic Peninsula clockwise through to the Ross Sea, the Ocean's around Antarctica show 50-70% probabilities of above-normal precipitation (figure 8). The remaining Amundsen / Bellinghausen Sea region, particularly north of 60S, however shows a 40-50% probability of below-normal precipitation for the JJA period. 40-60% probabilities of above-normal precipitation extend across the entire Antarctic Peninsula and East Antarctic-Atlantic region. 40-50% probabilities of above normal precipitation occur over the high interior and closer to the coast between 130E clockwise through to 130W. 40-50% probabilities of below-normal precipitation are indicated in the East Antarctic interior between 60-110E, particularly for July.

Information on the skill of the MME forecast for the surface air temperature and precipitation is provided in Annex 2. It appears that overall, the Antarctic Polar region generally has poorer forecast skill than most other parts of the globe. For JJA SAT's, there's some weak skill in the Pacific region between the Ross Sea and the Antarctic Peninsula, but for precipitation skill is generally poor across most of the continent.

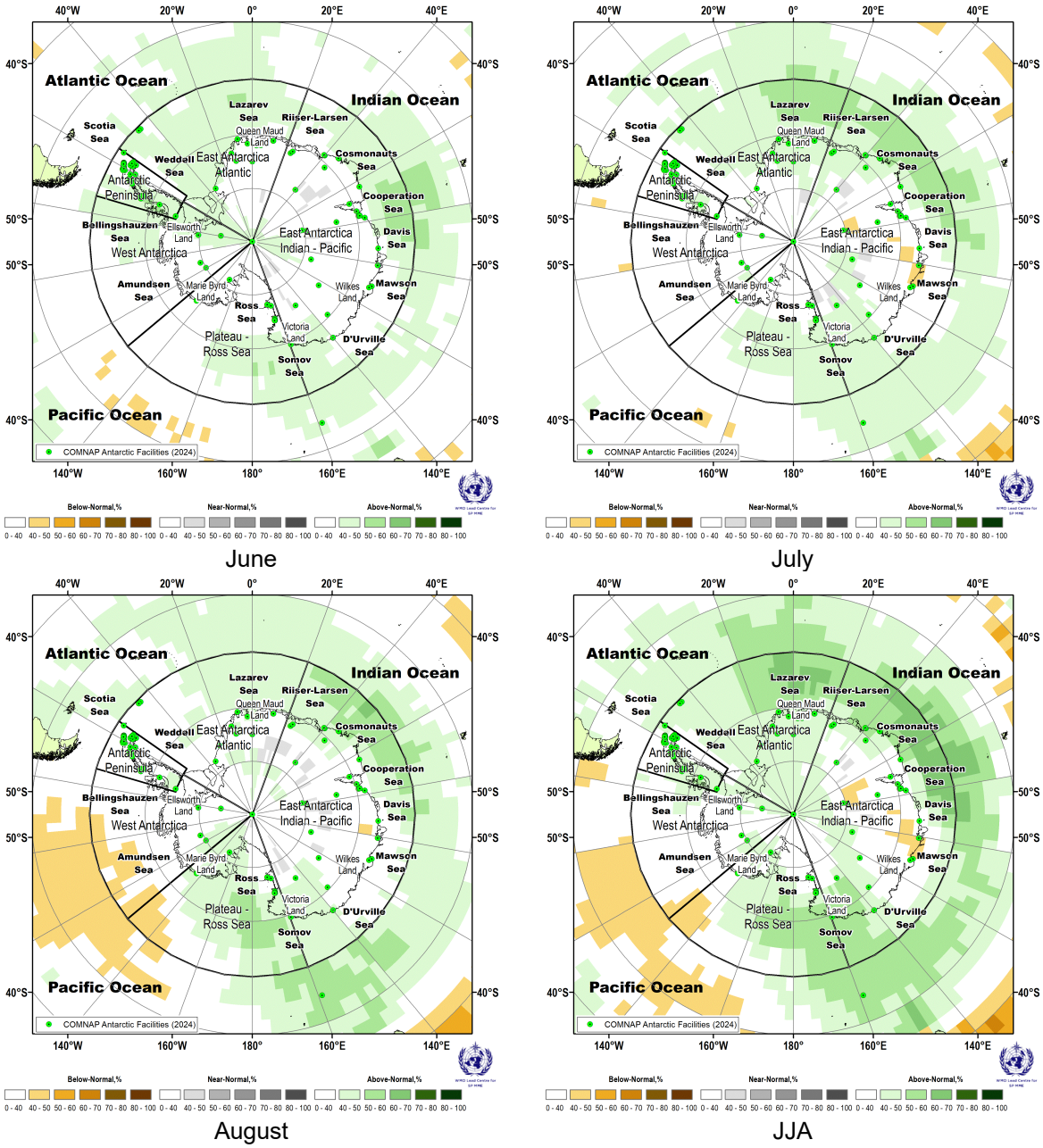

Figure 8 – Surface precipitation anomaly (relative to 1991-2020 period) seasonal probabilistic outlook for June, July, August and JJA 2026. Data source: WMO Lead Centre for Seasonal Prediction Multi-Model Ensemble (wmolc.org) forecast (11 GPCs-SP models) using data of 14 May 2026, graphics produced by AARI.

Sea-ice

Summary

Routine monitoring of sea-ice parameters in the Southern Ocean in the form of ice charting including mapping of ice shelfs and icebergs, was started from the time of the International Geophysical Year (IGY) in 1957. Introduction of operational satellite multichannel passive microwave techniques in October 1978 provided capability to track variability of sea-ice total concentration and ice drift patterns, and such derivative variables as ice extent, area and ice edge on a true circumpolar scale with 1-2 days periodicity. Recent advances in remote sensing

complemented the list of observed sea-ice variables, though mostly in winter, with ice thickness, ice age and stage of melt. Direct observations of sea-ice parameters which are provided at coastal stations, during expeditionary surveys, shipborne and by ice-strengthened lagrangian buoys, though very unevenly distributed in space, are extremely significant for regional climatologies and verification of remote sensing and numerical reanalysis.

Seasonal review: November 2025 – April 2026

Sea-Ice Extent

During late spring – summer – early autumn 2025/26, the overall Southern Ocean sea-ice extent continued to be in the relatively low state that has been observed since 2016 with sea-ice extent in the lowest percentiles in most of the parts of the Indian and Pacific sectors of the Southern Ocean (e.g. Bellingshauzen Sea). However, the opposite situation occurred in some of the seas of the Atlantic and Pacific sectors (e.g. West Weddell Sea), as apparent in Figure 9.

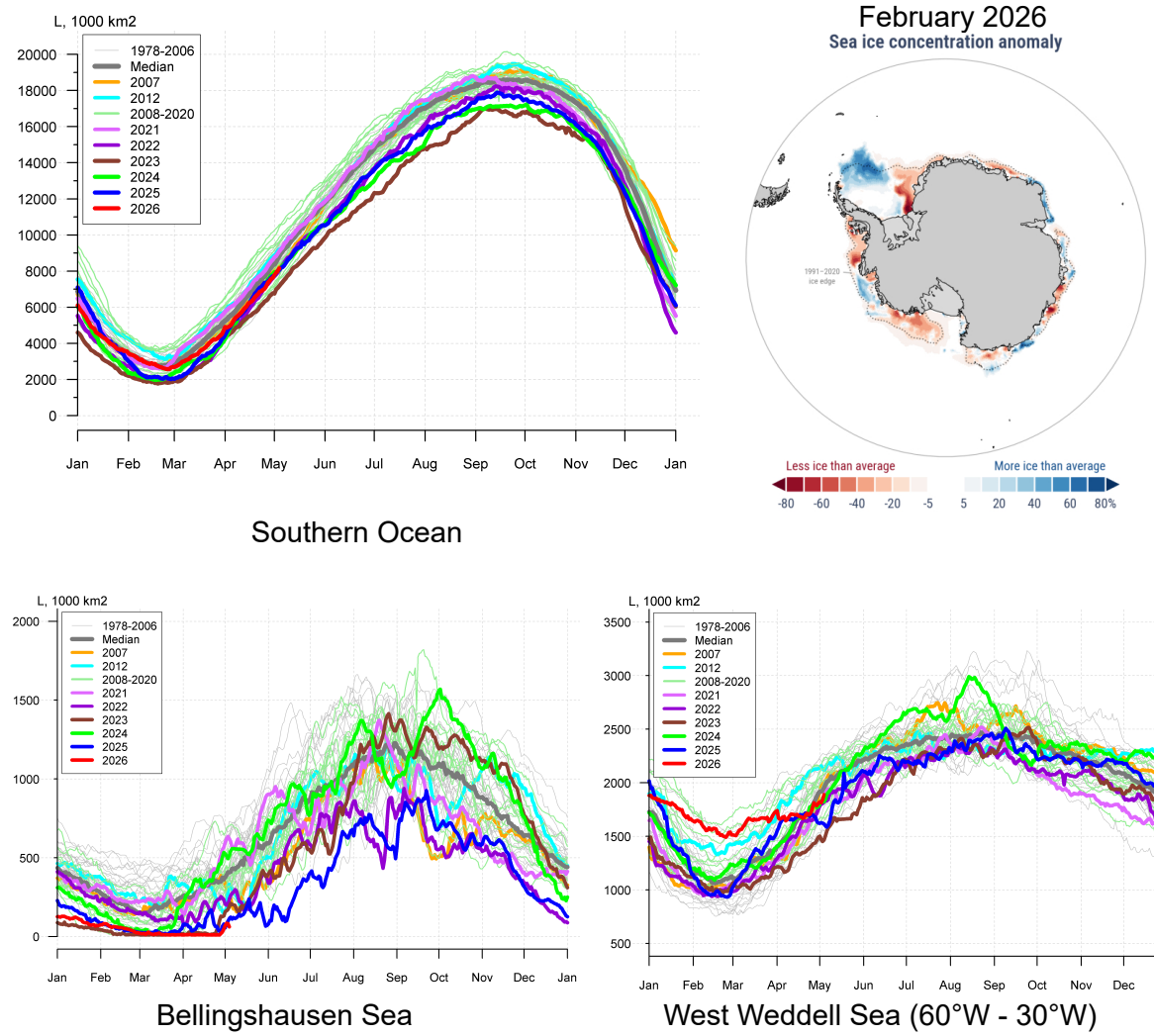

Figure 9 – Daily sea-ice extent in the Antarctic (top left) and selected Antarctic seas (Bellingshausen Sea, bottom left; West Weddell Sea, bottom right) for 1979-2026 period. Data source: NSIDC, graphics produced by AARI. February 2026 average sea-ice concentration anomaly (top right) relative to 1991-2020 period, credit: C3S/ECMWF.

The annual minimum sea-ice extent was reached during 22-26 February with a total area close to 2.6-2.8 million square km, ranking close to 16th lowest on record for the period 1979-2026 with the first two lowest occurring in 2022 and 2023 (2.0 million square km). This value is also by 1.0 million square km less than the maximum summer sea-ice extent observed in late February 2008 (3.7 million square km).

Sea-Ice Concentration

Seasonal anomalies in Antarctic sea-ice concentration (SIC) during 2025–2026 exhibited strong regional variability (Figure 10a). During austral spring (SON 2025), negative SIC anomalies dominated much of the Riiser-Larsen Sea, Cosmonaut Sea, and Cooperation Sea in the Indian Ocean sector, as well as the Bellingshausen Sea in the eastern Pacific sector, indicating reduced sea-ice concentration relative to climatology. In contrast, positive anomalies were observed in parts of the Lazarev Sea in the Atlantic sector, as well as the D'Urville Sea and Somov Sea in the western Pacific sector. During austral summer (DJF 2025/2026), below-average SIC was observed in the Bellingshausen Sea and Ross Sea, while pronounced positive SIC anomalies developed in the Weddell Sea in the Atlantic sector and the Amundsen Sea in the Pacific sector. In March–April 2026 (MA), negative SIC anomalies became widespread across much of Eastern Antarctica, while positive anomalies remained concentrated in parts of the Weddell Sea and Amundsen Sea.

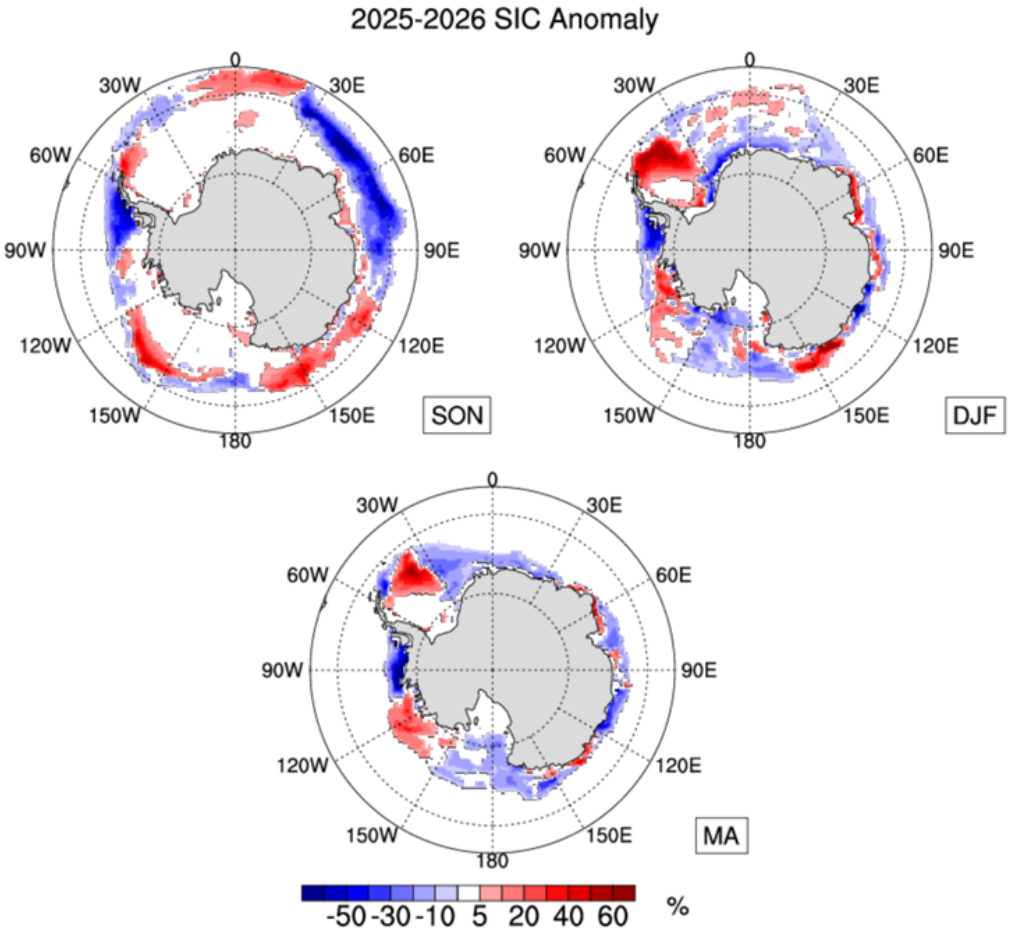

Figure 10a – Seasonal sea ice concentration anomalies (relative to 1991-2020, unit: %) in the Antarctic. Source: NSIDC and Fengyun satellite products, graphics provided by CMA.

Sea-Ice Conditions

Special features of the seasonal variability of the sea-ice conditions included southmost position of the ice edge during the spring melt (November – December 2025) in the seas of the Indian sector and eastern part of the Pacific sector with opposite northmost ice edge position foe Weddell, Lazarev and eastern Ross seas (Figure 10). During the peak of austral summer (January – February 2016) drastic reduction of sea-ice was observed in most of the areas of Indian and Pacific sectors (Figure 10) with open water in the Bellingshausen, East Weddell and Ross seas with opposite close or higher than median ice cover in West Weddell and Amundsen seas. Similar southmost position of the ice edge was observed within these seas during the start of the freezing period (March – April 2026) with notable exception again for the West Weddell and Amundsen seas. The sea-ice concentration pattern also depicts alternate positive and negative anomalies, indicating a wave-3 structure.

Total area of the Southern Ocean icebergs (mostly driven by the area of the very large icebergs monitored by the US National Ice Center) gradually decreased from 16.4 (21/11/2025) to 12.4 (03/04/2026) thousand square km due to destruction and fast melt of the champion in area A23A iceberg (3643 square km on 13 December 2024 to 140 square km on 20 March 2026) in the area of the South Georgia island (figure 10) with the D15A (3037 km^2 on 8 May 2026) as constantly the largest.

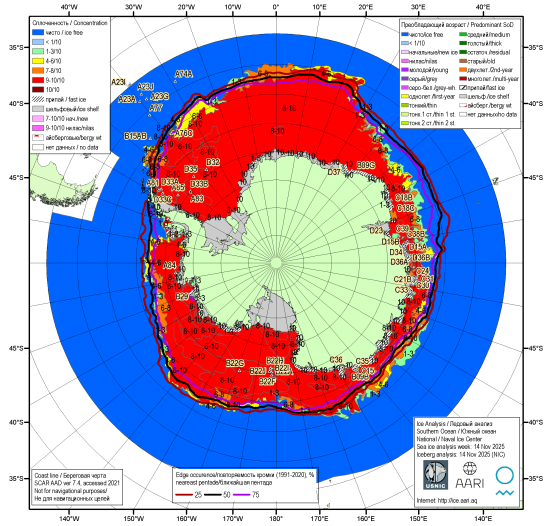

14 November 2025

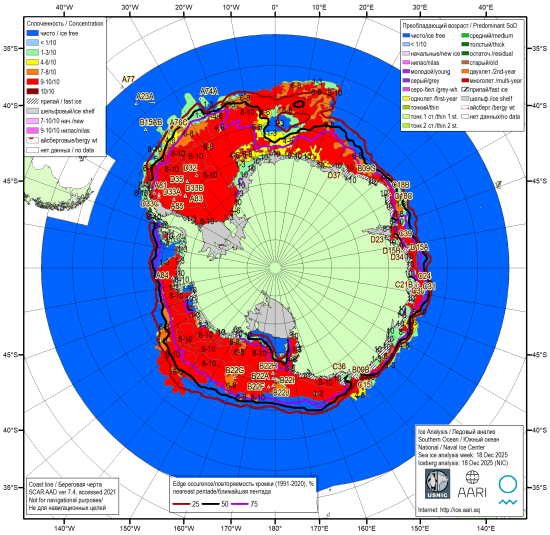

18 December 2025

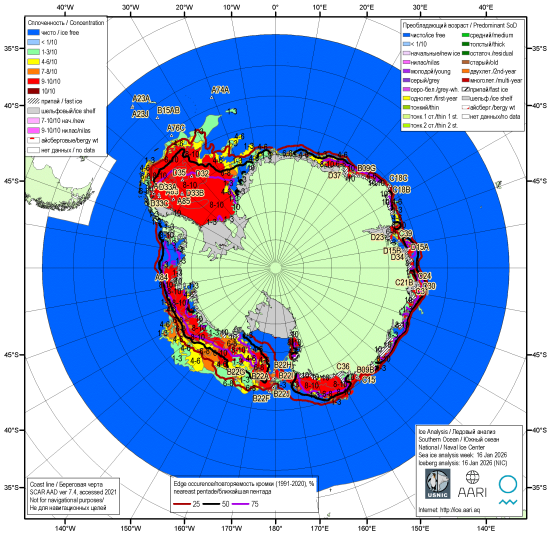

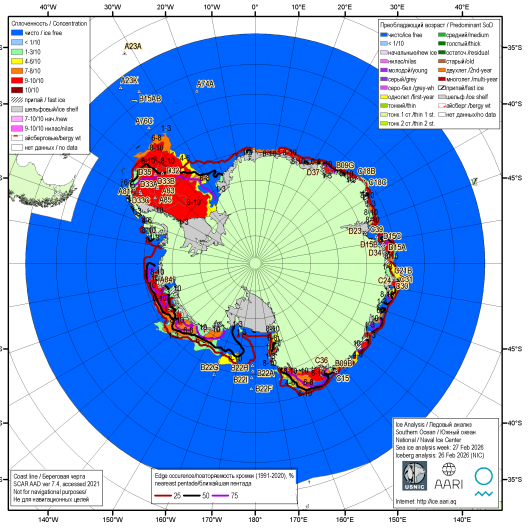

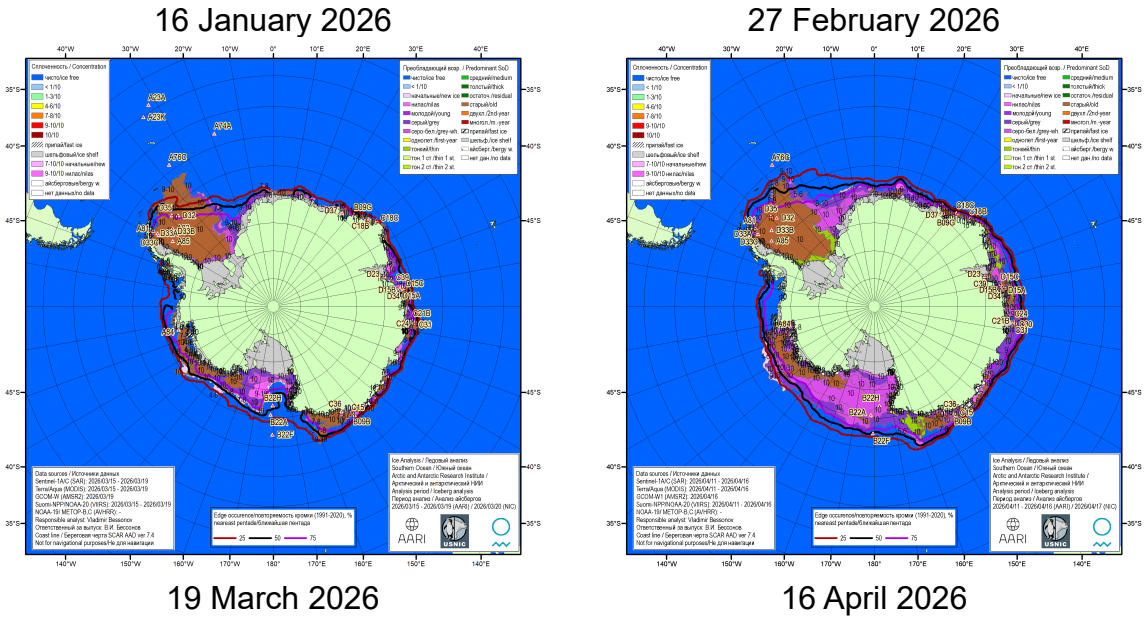

Figure 10b – Seasonal sea ice conditions in the Southern Ocean. Data source: AARI and US NIC (ice charting) and US NIC (large icebergs analysis), graphics produced by AARI. Colour coding (WMO/TD-No. 1215): 14/11 - 27/02 – based on sea-ice total concentration, 19/03 and 16/04 – based on sea-ice predominant stage of development.

Verification of summer 2026 sea ice forecast

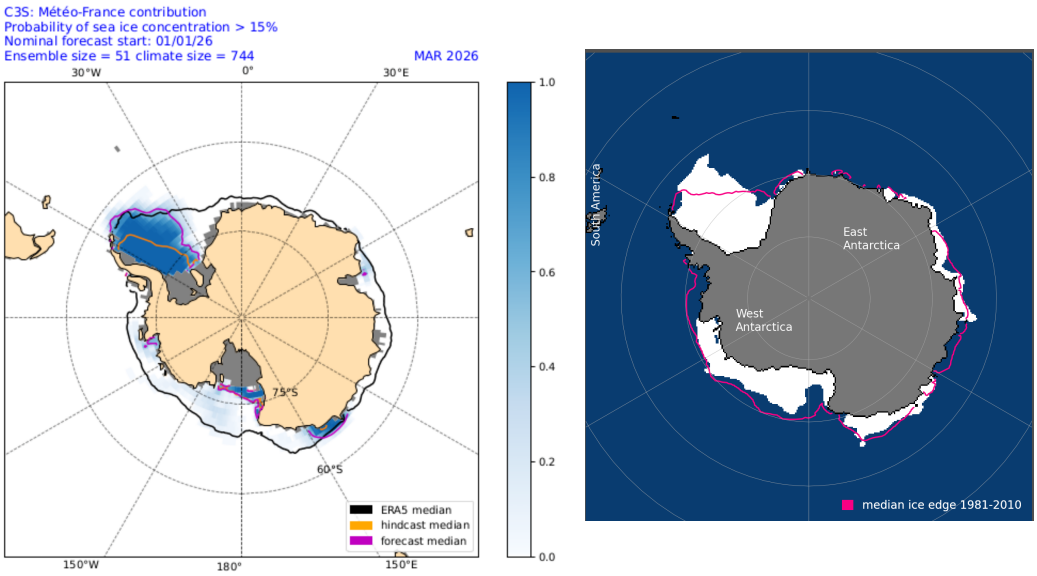

Figure 11 – Sea-ice concentration March 2026 multi-model ensemble probabilistic outlook (left) and passive microwave average monthly ice extent (right). Data source: outlook - Copernicus C3S System; CMCC, DWD, ECMWF, JMA, Météo France, UK Met Office monthly probability of SIC values > 15%, graphics produced by Météo France, analysis – NSIDC G02135 dataset.

Subjective comparison of the March 2026 MME probabilistic outlook and corresponding observed sea-ice extent shows quite good correspondence with the observed ice edge position in the Weddell, Cosmonauts, D'Urville, Ross and Amundsen seas (Figure 11). The Davis Sea (90E) area saw more ice than predicted

Seasonal Outlook: September 2026

Sea Ice predictions for September 2026 display a wide latitudinal spread (ie. where the forecast ice edge position has the most uncertainty) in the Pacific and Atlantic sectors running clockwise from 150W to 30E. Slight positive ice concentration anomalies relative to the ERA5 median 1991-2020, and subsequently a more northern ice edge position and increased extent, are predicted for the Pacific and Atlantic Regions (Weddell Sea).

Negative ice concentration anomalies, with reduced extent and a more southward position of the ice edge are predicted for the Indian Ocean Region (Cooperation and Davis seas). A weak dipole of ice concentration anomaly is represented in the Pacific (Ross Sea) Region at 160E and 150W.

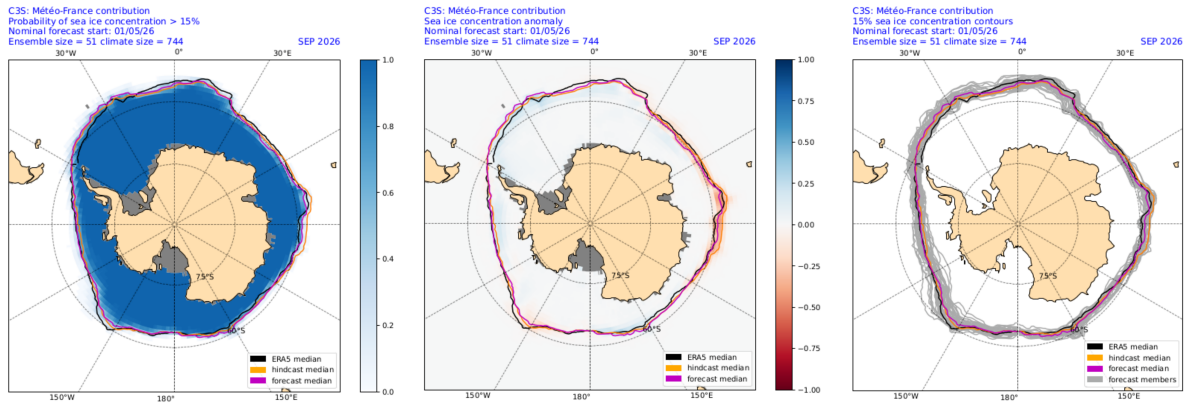

Figure 12 – Sea-ice concentration September 2026 multi-model ensemble outlook. Left: probability of SIC > 15%, middle: SIC anomaly, right: ensemble members. Data source: Copernicus C3S System, ECMWF, graphics produced by Météo France.

Polar ocean and glaciers surface heat balance

Seasonal review: November 2025 – April 2026

Surface layer ocean and land temperature variability (presented as a combined polar ocean sea surface temperature (SST) and soil/glacier ice surface layer 28-100 cm temperature (STL3) plot on figure 13) closely correlates with surface air temperature (see Figure 3).

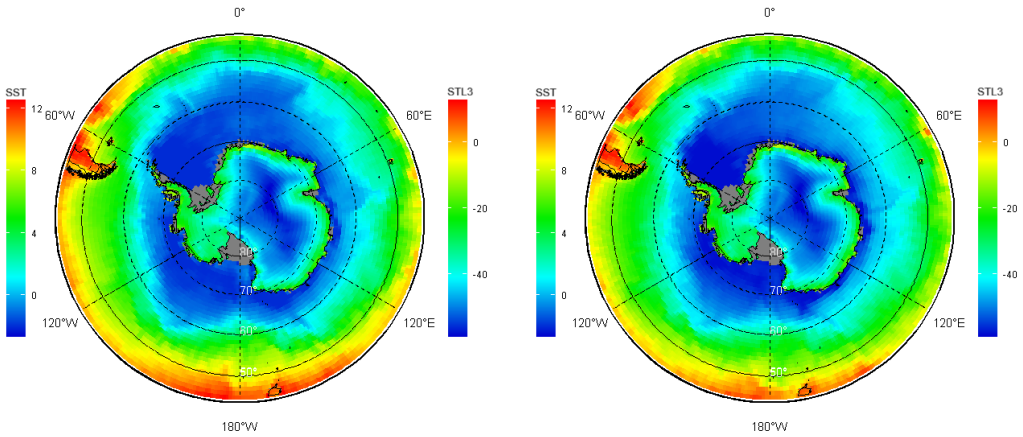

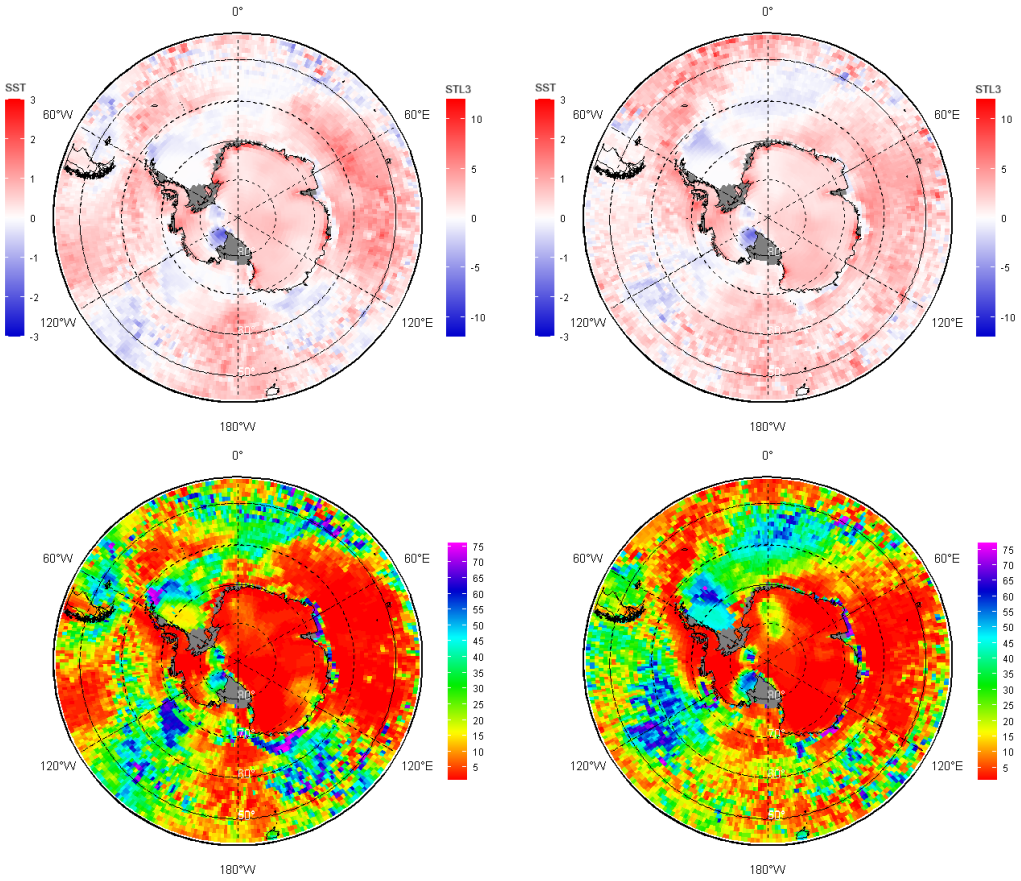

Figure 13 – Combined polar ocean sea surface temperature (SST) and soil/glacier ice surface layer 28-100 cm temperature (stl3) seasonal averages, anomalies (relative to 1991-2020) and ranks (relative to 1950-2024/2025). Data source: ERA5, graphics produced by AARI.

During the past season negative SST anomalies are identified for Amundsen, Scotia, Somov and Weddel seas with strong positive anomalies in the Indian and eastern Pacific sectors from Riiser-Larsen to D'Urville seas and Bellingshausen Sea (Figure 13). For the land Antarctic negative anomalies of the glacier ice surface layer are identified only for the areas of the Transantarctic Mountains and Plateau – Ross Sea sector. Other parts of the continent including the area of the 'Doomsday' Thwaites Glacier in the Marie Byrd Land are characterized by the prominent positive heat anomalies (Figure 13).

Seasonal Outlook – Sea Surface Temperature: June to August 2026

The outlook for JJA 2026 indicates above 70% probabilities of above normal SST in the open Oceans north of the sea ice zone. The veracity of the SST forecast under the Sea Ice Zone is questionable.

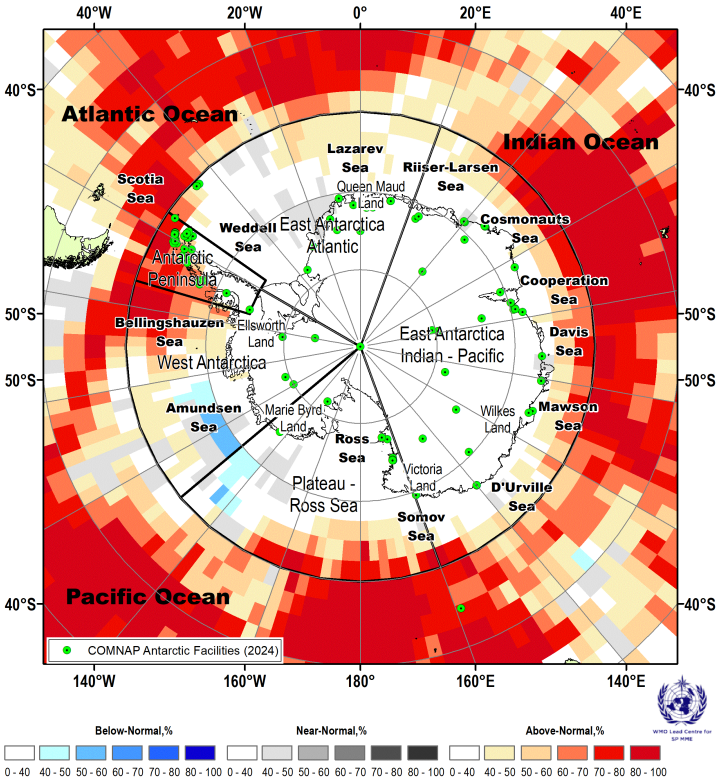

Figure 14 – Sea surface temperature anomaly (relative to 1991-2020 period) seasonal probabilistic outlook for JJA 2026. Data source: WMO Lead Centre for Seasonal Prediction Multi-Model Ensemble (wmolc.org) forecast (11 GPCs-SP models) using data of 14 May 2026, graphics produced by AARI.

Extremes

The analysis of temperature extremes can be explored by linking it to the frequency distribution of value measured at ground-based stations. Compared to the ranking, which is based on monthly and seasonal mean values determined by reanalysis since 1950, this type of analysis allows for a broader perspective on the daily temperature scale, while simultaneously making it less dependent on the absolute temperature value. For this purpose, a recently proposed methodology can be usefully employed (Bromwich et al., 2026[1]).

This methodology, based on the frequency distribution of maximum and minimum values for each day of the year, identifies extreme cases for a period whenever the maximum value recorded on a particular day of that period is greater than the 90th percentile of the frequency distribution. Conversely, for cold extremes, an event is identified whenever the daily minimum temperature falls below the 10th percentile. Table 2 below provide the results of this analysis applied to 28 selected meteorological observation stations distributed over the Antarctica continent, the most of them staffed stations.

Applied to observations at Amundsen-Scott station, this methodology indicates that for the period September 2025 – April 2026 extreme temperatures events have occurred with a frequency ranging between the lowest value of 3% in summer (DJF) and the highest value of 16% in autumn (MAM). These values are lower as expected, compared to the historical records, considering that the current period is characterized by neutral/slightly negative monthly and seasonal anomalies. Complementary analysis of cold extremes events, reveals

1Bromwich, D.H., Zou, X. & Wang, SH. Interior Antarctica is undergoing marked climate change. *Commun Earth Environ* **7**, 389 (2026). https://doi.org/10.1038/s43247-026-03384-4.

that they occurred with the lowest frequency of 2% in autumn and the highest frequency of 28% in summer.

In contrast for the Mawson station located in the East Antarctic area and characterized during the current period by higher-than-average monthly temperatures with seasonal temperatures near to the record, extremes temperatures events have occurred with a frequency between 40% in spring and 19% in autumn with the lowest value of 9% in summer. During the same period cold extremes were instead very few (near 0%).

Table 2 – Percentage of WARM events along the period September 2025 – April/May 2026 at selected stations, most of them staffed, located over the Antarctic Continent. Analysis is performed making use of or adapting the methodology proposed by Bromwich et al, 2026. The number for WARM events provides % of days with T_{max} above the 90th percentile. Values above 10% are highlighted in red, and values above 20% in bold red. The number of COLD events provides % of days with T_{min} below the 10th percentile. Valuers above 10% are highlighted in blue and values above 20% in bold blue.

Station	WARM			COLD		
	SON	DJF	MAM	SON	DJF	MAM
Amundsen-Scott	4.4	3.3	16.1	4.4	**27.8**	1.6
Belgrano-II	18.7	0.0	8.8	8.8	11.1	7.5
Byrd	11.0	3.3	**23.0**	4.4	13.3	6.6
Casey	5.5	16.7	17.6	4.4	2.2	14.9
Concordia	14.3	**23.6**	15.5	0.0	3.4	2.8
Davis	**35.2**	5.6	12.2	0.0	4.4	0.0
Dumont-Durville	**22.0**	**21.1**	13.5	4.4	5.6	17.6
Eneide	6.6	**21.1**	10.5	0.0	0.0	0.0
Esperanza	8.8	16.7	**20.3**	13.2	12.2	2.7
Faraday-Vernadsky	7.7	18.9	**26.0**	0.0	2.2	0.0
Great Wall	14.6	**21.1**	13.0	11.2	10.0	1.9
Halley	16.5	2.2	2.7	5.5	6.7	13.3
King Sejong	11.0	17.8	**22.8**	11.0	11.1	3.8
Marambio	9.9	7.8	12.7	**20.9**	6.7	2.5
Mawson	**38.5**	8.9	19.0	0.0	11.1	0.0
McMurdo	14.3	12.2	11.4	2.2	11.1	5.1
Mirny	17.6	17.8	17.7	4.4	5.6	7.6
Neumayer	18.7	2.2	2.5	5.5	12.2	5.1
Novolazarevskaya	**33.0**	5.6	14.6	4.4	13.3	4.9
Orcadas	6.6	5.6	**22.8**	14.3	11.2	2.5
Palmer	8.8	11.2	**20.7**	0.0	4.5	0.0
Rothera	14.3	**29.2**	**20.7**	0.0	4.5	1.2
San Martin	11.0	**22.2**	14.6	0.0	5.6	1.2
Scott Base	16.5	18.9	18.8	2.2	2.2	2.1
Syowa	**34.1**	6.7	**23.2**	2.2	2.2	0.0
Troll	N/A	N/A	**20.4**	N/A	N/A	0.0
Vostok	**30.8**	14.4	**20.7**	0.0	13.3	11.0
Zhongshan	**36.3**	**25.6**	**22.0**	4.4	7.8	4.9

Data sources and useful links

(under development)

Australian Antarctic Program
Arctic and Antarctic Research Institute (PRCC resources)
Australian Government Bureau of Meteorology
Copernicus Climate Change Service
- ERA5 monthly averaged data on pressure and single levels (ERA5)
- Marine environment monitoring service (CMEMS)
- Seasonal forecast

Danish Technical University (sea ice portal)
Finnish Meteorological Institute
Alfred Wegener Institute
National Snow and Ice Data Center (NSIDC)
Norwegian Meteorological Institute (Cryo service)
US National Ice Center (Antarctic home)
WMO Arctic Regional Climate Centre - Network (ArcRCC-N)
WMO Global Cryosphere Watch (GCW)
WMO Lead Center for Long-Range Forecast Multi-Model Ensemble
- Seasonal MME forecast

Background and contributing institutions

The Antarctic seasonal climate summary and outlooks were prepared for AntCF-2 in partnership between the AARI, AMRDC, BAS, BOM, CMA, CNR, Met Office, NCPOR, NOC, SAWS, SMN and UNI-Chieti.

Acknowledgements

Writing team: Scott Carpentier (BoM), Steve Colwell (BAS), Piero Dicarlo (CNR), Christopher Hewitt (NOC), Matthew Lazzara (AMRDC), Nuncio Murukesh (NCPOR), Chiara Pambianco (UNI-Chieti/CNR), Anastasiia Revina (AARI), Vasily Smolyanitsky (AARI, editor), Vito Vitale (CNR).

The authors acknowledge the Council of Managers of National Antarctic Programs (COMNAP) and its Member National Antarctic Programs, whose sustained logistical, operational, and scientific support underpin the observations, data, and infrastructure used in this Statement. Many of the datasets, observing systems, and facilities referenced here are made possible through national Antarctic programme investments and coordination.

Special acknowledgement and gratitude are to Chiara Pambianco, University “Gabriele D'Annuncio” of Chieti-Pescara, for design of the Antarctic Climate Forum unique logo.

Acronyms

AAP	Australian Antarctic Program
AARI	Arctic and Antarctic Research Institute (Russian Federation)
ACF	Arctic Climate Forum
AMRDC	Antarctic Meteorological Research and Data Center, SSEC
AntRCC-N	Antarctic Regional Climate Centre Network
ArcRCC-N	Arctic Regional Climate Center Network
AntCF	Antarctic Climate Forum
AWI	Alfred Wegener Institute for Polar Research (Germany)
BAS	British Antarctic Survey
BOM	Australian Government Bureau of Meteorology
CAP	Common Alerting Protocol
CCCS	Copernicus climate change service
CMA	Chinese Meteorological Administration
CMEMS	CCCS Marine environment monitoring service
CNR	Consiglio Nazionale delle Ricerche (National Research Council) (Italy)
COMNAP	Council of Managers of National Antarctic Programs
ECMWF	European Centre for Medium-Range Weather Forecasts
ESA	European Space Agency
GCW	WMO Global Cryosphere Watch program
GPCs-LRF	WMO Global Producing Centres Long-Range Forecasts
GloSea5	Met Office Global Seasonal forecasting system version 5
H50, H500	Geopotential heights 50hPa, 500hPa
HYCOM-CICE	HYbrid Coordinate Ocean Model, Coupled with sea-ice
IICWG	International Ice Charting Working Group
IOC	Intergovernmental Oceanographic Commission
LC-LRFMME	WMO Lead Centre for Long Range Forecast Multi-Model Ensemble
MSLP	Mean sea level pressure
NIC	National Ice Center (United States)
NCAR	National Center for Atmospheric Research (United States)
NCAR CFSR	National Center for Atmospheric Research Climate Forecast System Reanalysis
NCPOR	National Centre for Polar and Ocean Research (India)
NMI	Norwegian Meteorological Institute
NOAA/NWS	National Oceanic and Atmospheric Administration/National Weather Service (United States)
NCEP/CPC	National Centers for Environmental Prediction/Climate Prediction Center (United States)
NOC	National Oceanography Centre (UK)
NSIDC	National Snow and Ice Data Center (United States)
MME	Multi-model ensemble
RCC	WMO Regional Climate Centre
RCOF	Regional Climate Outlook Forum
SAT	Surface air temperature
SAWS	South African Weather Service
SCAR	Scientific Committee on Antarctic Research
SIC	Sea-ice concentration
SIE	Sea-ice extent
SIT	Sea-ice thickness
SMN	Servicio Meterologico Nacional (National Meteorological Service) (Argentina)
SSEC	Space Science and Engineering Center of University of Wisconsin-Madison (United States)
SST	Sea surface temperature
SWE	Snow Water Equivalent
UNI-Chieti	University “Gabriele D'Annunzio” of Chieti-Pescara (Italy)
WIS	WMO Information System
WMO	World Meteorological Organization

Annex 1 – Micro Rain Radar at Great Wall Station

The Micro Rain Radar (MRR; K-band,24GHz) deployed at China's Antarctic Great Wall Station (62°13′ S, 58°58′ W; 10 m a.s.l.) has been operating since early 2024. The instrument is a vertically pointing frequency-modulated continuous-wave (FM-CW) Doppler radar system. Except for two short data gaps caused by an SD-card malfunction, namely 23–27 August 2025 and 10 September 2025, which are indicated by grey hatched areas in Figure 1, the MRR record is essentially continuous. During the period from 10 March 2024 to 28 February 2026, a total of 715 days of effective observations were obtained.

During the observation period, the MRR was operated with a native temporal resolution of 10 s and a vertical resolution of 35 m, with a maximum observational height of approximately 4.45 km above ground level. For each time step and range gate, the raw Doppler spectrum was recorded with 64 spectral bins. The maximum unambiguous Doppler velocity was approximately 11.89 ms^{-1}. Owing to near-field effects and possible ground-clutter contamination, the lowest usable range gate for snowfall statistics was approximately 300 m above ground level. All MRR Doppler spectra were processed using a Doppler-spectra-based framework following Maahn and Kollias (2012). This processing framework applies robust noise suppression and a dynamic dealiasing strategy, thereby improving the retrieval of weak spectral signatures, including subtle vertical-motion signals. It is designed to enhance data quality under the low signal-to-noise conditions typical of snowfall, to obtain reliable radar measurements, and to increase the sensitivity of the instrument to snowfall.

About MRR observation and analysis it is also useful to refer to the Appendix to the 1st Consensus Statement Report.

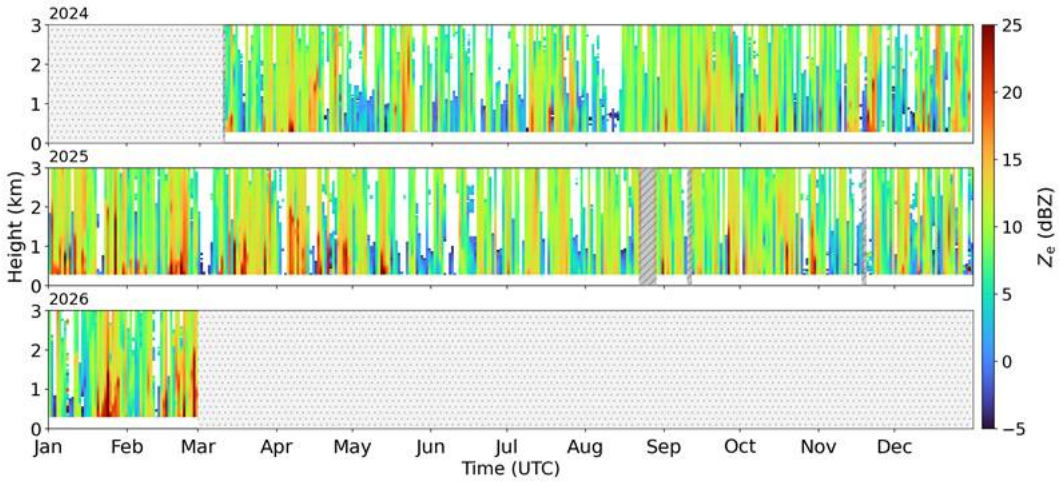

Annex Figure 1 - Daily mean profiles of MRR equivalent radar reflectivity (Ze) at Great Wall Station. Grey hatched areas denote periods with missing data.

Maahn, M. and Kollias, P.: Improved Micro Rain Radar snow measurements using Doppler spectra post-processing, Atmos. Meas. Tech., 5, 2661–2673, https://doi.org/10.5194/amt-5-2661-2012, 2012.

Annex 2 – WMO LC-LRFMME skill assessment

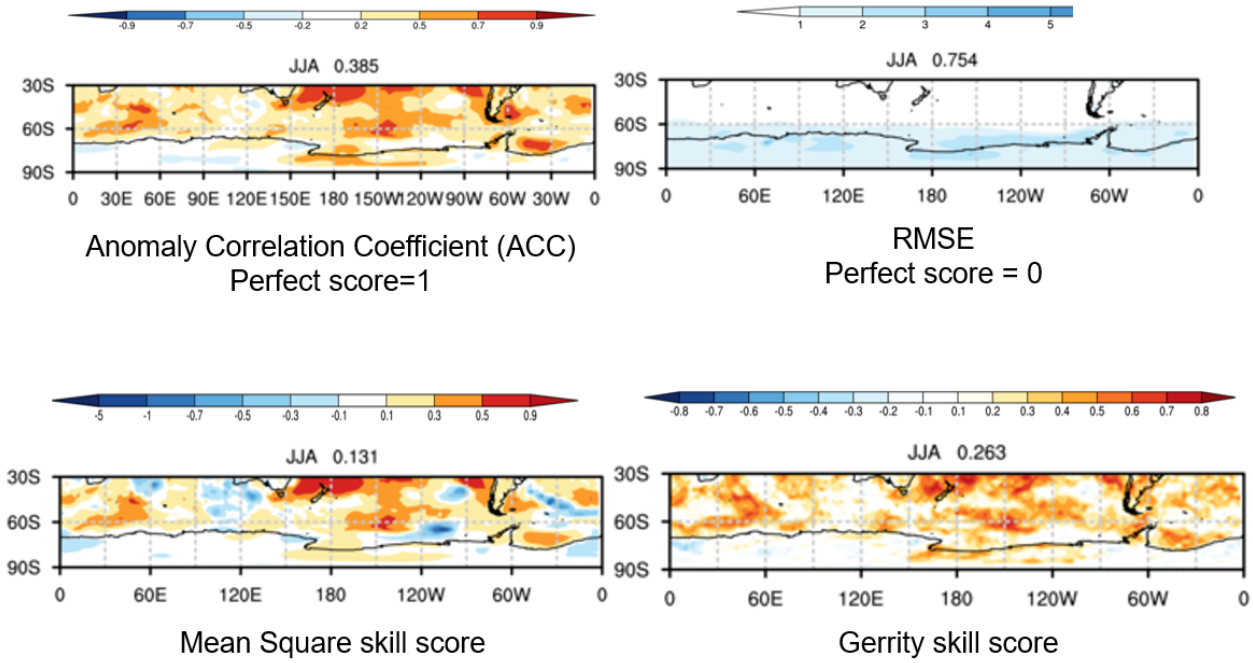

Anomaly Correlation Coefficient (ACC)
Perfect score=1

RMSE
Perfect score = 0

Mean Square skill score

Gerrity skill score

Annex Figure 2 - Surface air temperature (2m) hindcast (1993-2009) skill assessment for JJA MME deterministic, source – WMO LC-LRFMME (wmolc.org).

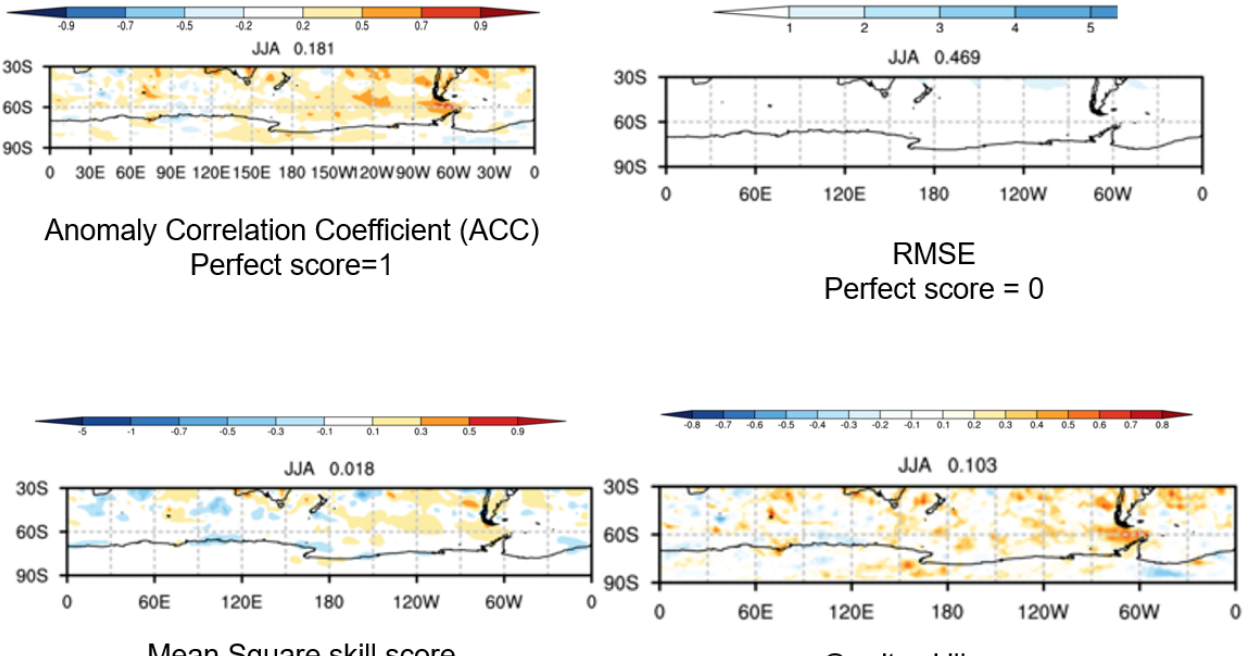

Anomaly Correlation Coefficient (ACC)
Perfect score=1

RMSE
Perfect score = 0

Mean Square skill score

Gerrity skill score

Annex Figure 3 – Surface precipitation hindcast (1993-2009) skill assessment for JJA MME deterministic, source – WMO LC-LRFMME (wmolc.org).